Mechanical properties and fracture characteristics of $W_f/Cu_{82}Al_{10}Fe_4Ni_4$ composites

YANG CHUN MEI[a], ZHANG YANG[*,b], WU ZHE[a], MA YAN[a], LIU QIAN JUN[a]
[a]*College of Mechanical and Electrical Engineering, Northeast Forestry University, Harbin 150040, China*
[b]*College of Science, Northeast Forestry University, Harbin 150040, China*

Tungsten fiber reinforced $Cu_{82}Al_{10}Fe_4Ni_4$ composites were fabricated by penetrating casting method. Mechanical properties and fracture characteristics of the composites were discussed by tensile test and bending test. The microstructure and fracture characteristic were investigated by Transmission electron microscopy(TEM) and Scanning electron microscopy(SEM). Microstructure observation of $W_f/Cu_{82}Al_{10}Fe_4Ni_4$ composites revealed that a small amount of tungsten diffused into the Fe–Ni solid solution precipitated on the surface of tungsten fibers. The interface of the composite remained good after tensile test and bending test. The experimental results showed that the interface between tungsten fibers and matrix alloy was compact, and the interface exhibited high strength under pull and bending force. The composites occurred brittle fracture in tensile test, and tensile strength was 1300Mpa. The composites also occurred brittle fracture in bending test, and bending strength was 1540Mpa.

(Received December 3, 2013; accepted October 28, 2015)

Keywords: $W_f/Cu_{82}Al_{10}Fe_4Ni_4$ composites, Microstructure, Interface, Mechanical properties

1. Introduction

With the development of armor-piercing projectile to high speed, high strength and high density, the demand of mechanical properties of the materials used for armor-piercing projectile increased higher and higher [1-3]. Composites are composed of two or more kinds of material reasonably, so they often possess better performance than a single material. Therefore, many countries start to do research in composites' armor-piercing projectile in recent years [4-6]. Tungsten fibers, which possess the advantages of high density and high melting point (3410℃), were formed by drawing the massive tungsten at high temperature [7-9]. During the process of drawing, the internal microstructure of the tungsten fibers were drawn into be fibrous so that the tungsten fibers could obtain high mechanical properties [10,11]. Due to the above advantages, tungsten fibers are selected as a reinforcement for the new generation of composites used in armor-piercing projectile [10]. As copper alloy possesses the properties of high density and high strength, and tungsten-copper composites have been successfully used in electronics, military and aerospace fields, so that copper alloy was chosen as the matrix of the composites in this paper [12-15]. In order to increase the interface bonding strength, iron, nickel and aluminum elements were added in the copper, then $W_f/Cu_{82}Al_{10}Fe_4Ni_4$ composites were prepared by means of penetrating casting method [16]. Then the microstructure, interface strength and fracture mode of the composites are investigated in this paper.

2. Materials and experimental methods

$Cu_{82}Al_{10}Fe_4Ni_4$ alloy was chosen as the matrix and 0.25mm diameter straightening tungsten fibers were the reinforcement in $W_f/Cu_{82}Al_{10}Fe_4Ni_4$ composites. Tungsten fibers were cut into 200mm long and immersed in 40%HF liquor to remove the surface oxide film. Then tungsten fibers with pure surface will be gotten after cleaning in acetone and alcohol respectively by ultrasonics. The prepared tungsten fibers were put straightly into the clean quartz tube and the master alloy was set above the tungsten fibers, then $W_f/Cu_{82}Al_{10}Fe_4Ni_4$ composites was fabricated by means of flow casting method. The volume fraction of the tungsten fibers in the prepared composites is 80%. Tensile test samples with the demission of Φ8mm x 120mm, in which tungsten fibers arranged vertically, were prepared by means of wire cutting machine. Three-point bending samples with the dimension of 5mm ×5mm×35mm were made by the linear cutting machine. Then each group test will be tested for three times to ensure the reliability of the test data. Microstructure of $W_f/Cu_{82}Al_{10}Fe_4Ni_4$composites and fracture morphology after test were observed by scanning electron microscope (SEM).

3. Results and discussion

3.1 Microstructure observation

SEM microstructure at interface in $W_f/Cu_{82}Al_{10}Fe_4Ni_4$ composites was shown in Fig. 1a, from which interfacial

reaction products on the surface of tungsten fibers could be observed, and Energy Disperse Spectroscopy (EDS) insert showed tungsten, ferrum and nickel were the major elements of interfacial reaction products. Fig. 1b was TEM microstructure at interface in the composites, and the Selected Area Electron Diffraction Pattern (SADP) insert indicated that the interfacial reaction products were Fe-Ni solid solutions. The EDS and SADP analysis indicated that tungsten has diffused into Fe-Ni solid solutions at interface of $W_f/Cu_{82}Al_{10}Fe_4Ni_4$ composites. Tungsten and copper are not miscible, which causes that the interface bonding strength of the W-Cu composites is poor, and this kind of diffusion of tungsten into Fe-Ni solid solution is favorable to enhance the interface bonding strength of $W_f/Cu_{82}Al_{10}Fe_4Ni_4$ composites. In general, tungsten can react with nickel easily to generate Ni_4W brittle phases, which makes the interface strength of the composites become poor, but there were only Al_3Ni and AlFe intermetallic compounds in $W_f/Cu_{82}Al_{10}Fe_4Ni_4$ composites as shown in Fig.1c and d, indicating that nickel in $W_f/Cu_{82}Al_{10}Fe_4Ni_4$ composites existed as the form of Fe-Ni solid solutions and Al_3Ni intermetallic compounds in stead of Ni_4W brittle phases.

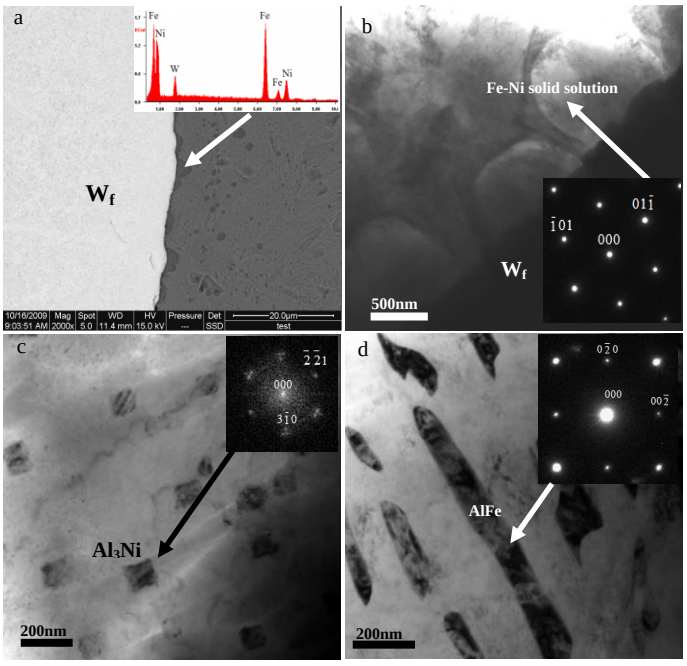

Fig. 1. Microstructure of $W_f/Cu_{82}Al_{10}Fe_4Ni_4$ composties. a) SEM image at interface in the composites, EDS insert shows the elements of interfacial reaction product; b) TEM image at interface in the composites, SADP insert shows interfacial reaction product is Fe-Ni solid solution; (c) and (d) TEM images of the composites in matrix, SADP insert in c) shows Al_3Ni intermetallic compound exists in matrix, SADP insert in d) shows AlFe intermetallic compound exists in matrix.

3.2 Tensile mechanical properties of the composites

Fig. 2 was the tensile stress-strain curve of $W_f/Cu_{82}Al_{10}Fe_4Ni_4$ composites. From Fig. 2, it could be observed that the stress-strain curve of composites was basically a straight line, and the tensile strength of the composites was 1300MPa. In the process of tensile test, the composites distorted due to loads bearing, and fractured eventually. This process generally included the following stages: The first stage was the elastic deformation stage of tungsten fiber and matrix alloy. Tensile stress-strain curve was a straight line at this time, and slope of curve acts as the elastic modulus of composites; the second stage was the stage of tungsten fiber elastic deformation and matrix alloy plastic deformation; the third stage was the fracture stage of tungsten fibers and matrix alloy. The strength and elastic modulus of tungsten fiber were much higher than $Cu_{82}Al_{10}Fe_4Ni_4$ alloy, and the volume fraction of tungsten fiber accounts for 80%, due to which, $W_f/Cu_{82}Al_{10}Fe_4Ni_4$ composites reflected more brittle fracture characteristics of tungsten fiber while under tensile force in the process from loads bearing to failure. So the performances of above second and third stages were not obvious, the final tensile stress-strain curve of composites showed typical linear relation, which was the brittle fracture characteristic of tungsten fiber reflected from $W_f/Cu_{82}Al_{10}Fe_4Ni_4$ composites in the process of bearing failure.

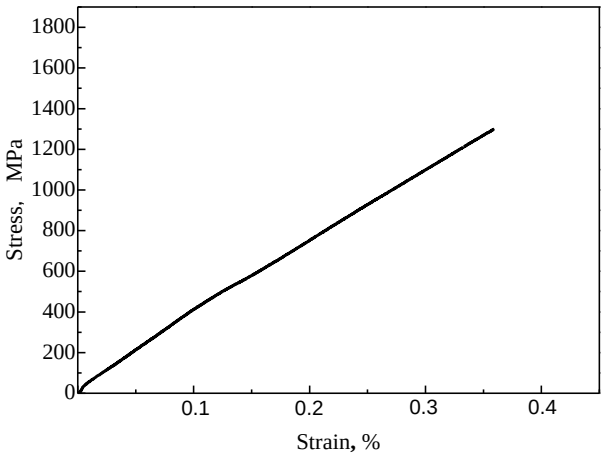

Fig. 2. Tensile stress-strain curve of the composites

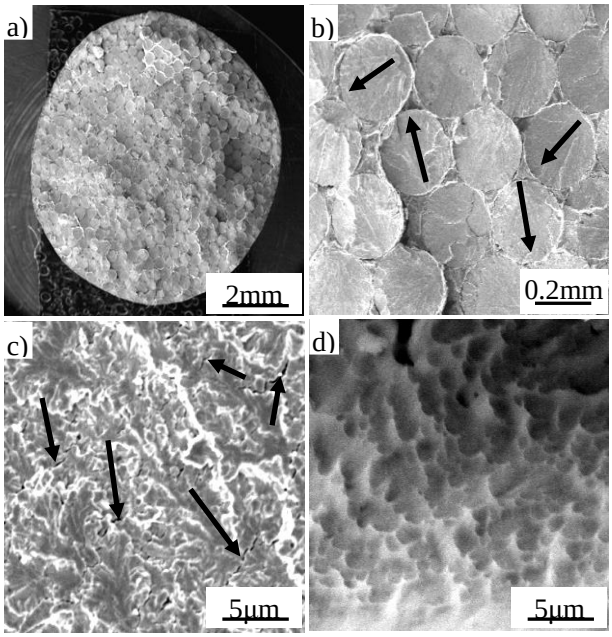

Fig. 3. Fracture morphologies of the composites a) Whole fracture surface b) Local fracture surface c) Micro cracks in single tungsten fiber d) Dimple fracture in Cu alloy

Fig. 3 a) was the total SEM observations of fracture morphologies of $W_f/Cu_{82}Al_{10}Fe_4Ni_4$ composites, from which we can observe that fracture was flat, and no tungsten fibers pulled out, only certain fluctuations in fracture local areas reflecting the brittle fracture characteristic. From local fracture surface enlarged Fig.3 b) it could be observed that combination condition of tungsten fiber and matrix was good, no obvious damage, and fracture surface of each tungsten fiber embodies river shape pattern, which indicated cleavage fracture of tungsten fibers while under tensile force, and according to the river course, the initial fracture location and extension direction coulded be found, as the arrows shown in the picture. For enlargement of single tungsten fiber fracture cracks as in 3 c), many cracks inside tungsten fibers could be observed. The cause of cracks inside tungsten fibers dued to that the plastic deformation ability of matrix was superior to tungsten fiber. Matrix alloy had a tendency to constriction when composites under tensile loads, but matrix and tungsten fiber interface were sticked together which restricts matrix constriction, if composites interface bonding strength was low at this time, interface damages would appear, and if composites interface bonding strength was high, interface would pass the contraction force to tungsten fiber to make it under force radially, which made tungsten fiber fracture radially. The results of Fig. 3 c) indicate radial fracture of tungsten fiber, which testified that $W_f/Cu_{82}Al_{10}Fe_4Ni_4$ composites surface had high intensity.

In SEM observations of matrix alloy on tensile fracture, the dimple fractures could be found after fracture of matrix alloy, as shown in 3 d). Usually, dimples are associated with the second phase particles in material, but in matrix Cu alloy of $W_f/Cu_{82}Al_{10}Fe_4Ni_4$ composites exist large amount of precipitated phases with large size, such as (Fe, Ni)、AlFe and Al_3N. When matrixes surrounded these precipitated phases have plastic deformations, and due to block of dislocation movement from precipitated phases, dislocation can only bypass precipitated phases and form a dislocation circle around precipitated phases. When the deformation increases, amount of dislocation around precipitated phases also increases. Dislocation will be under force from two aspects at this time: the first one is to push dislocation to precipitated phases under the action of dislocation source; the second is the blocking of precipitated phases will give a repulsive force to leading dislocation. When applied force is large enough, or strength value of top of dislocation pile-up group around precipitated phases reaches to a certain extent, micropores out of debonding may appear at the interface of precipitated phases and matrix. Because of the micropores, obstacles on top of dislocation pile-up group no longer exist, and dislocation at front disappear in cracks, while dislocation at rear loses front repulsive force, together with constant forward movement, which makes micropores continuously grow to form dimples.

3.3 Three-point bending mechanical properties of the composites

Fig. 4 was Bending stress-deflection curve of $W_f/Cu_{82}Al_{10}Fe_4Ni_4$ composites. Bending strength of composites was high, which reached to 1540Mpa. As shown from the Fig.4, the composites were in the stage of elastic deformation before damages, material strength presents a linear increase with the increase of deflection, no obvious plastic deformation, and when strength reached to maximum value, the material fails.

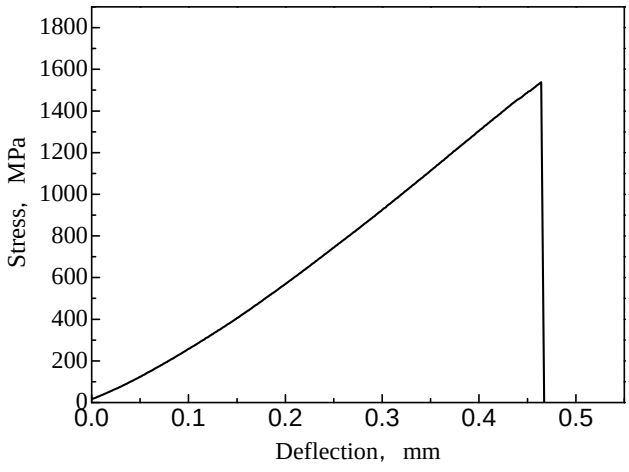

Fig. 4. Bending stress- deflection curve of $W_f/Cu_{82}Al_{10}Fe_4Ni_4$ composites

Fig. 5 was the total bending fracture morphologies of the composites. Although showing some ups and downs, from an overall aspect the fractures are flat and smooth, only a few tungsten fibers are pulled out, not with large amounts, and obvious brittle fracture characteristics are shown at the fractures. Fig. 5 b) and c) were enlarged pictures of local fracture surface, we can observe river shape pattern due to cleavage fracture of tungsten fiber, and tungsten fiber splittings as arrow shown in Fig. 5 b), but damages at the interface are less, which indicates that in the process of bending test, the composites surface strength is high. The observation of bending fracture also indicates dimple fractures after matrix alloy fractures, as shown in Fig. 5 d). From the analysis and of Bending stress- deflection curve of the composites and observation of fracture appearance, we can find that the damages of composites present brittle fracture characteristics, and the interface is the bonding of strong interfaces.

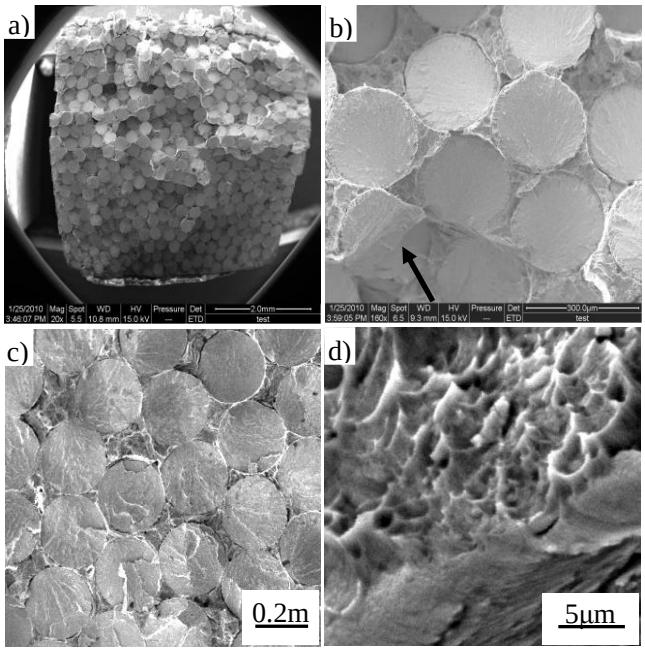

Fig. 5. Bending fracture morphologies of $W_f/Cu_{82}Al_{10}Fe_4Ni_4$ composites Whole fracture surface b) Local fracture surface c) Local fracture surface d) Dimple fracture

4. Conclusions

In $W_f/Cu_{82}Al_{10}Fe_4Ni_4$ composites, the internal fibrous microstructure of the tungsten fibers are kept well. A lot of Fe-Ni solid solution precipitated on the surface of tungsten fibers and tungsten would diffuse into Fe-Ni solid solution, which will improve the interface strength of the composites and make it to be provided with high strength and high plasticity. The experimental results also show that the interface between tungsten fibers and matrix alloy was compact, and the interface exhibited high strength under pull and bending force.

Acknowledgements

This material is based upon work supported by the Fundamental Research Funds for the Central Universities (grant no. 2572015DB02 and 2572015CB10) , the National Natural Science Foundation of China (grant no. 31200434) and the China Postdoctoral Science Foundation (No. 2013M531007).

References

[1] S. Pappu, C. Kennedy, L. E. Murr, L. S. Magness, D. Kapoor, Mater. Sci. Eng. A **262**, 115 (1999).
[2] F. M. Randrianarivony, S. Lair, S. A. Quinones, L. E. Murr, J. Mater. Sci. 37, 5197 (2002).
[3] J. X. Liu, S. K. Li, A. L. Fan, H. C. Sun, Mater. Sci. Eng. A **487**, 235 (2008) -242.
[4] R. D. Conner, R. B. Dandliker, W. L. Johnson, Acta Mater. **46**, 6089 (1998).
[5] H. F. Zhang, H. Li, A. M. Wang, H. M. Fu, B. Z. Ding, Z. Q. Hu, Intermetallics **17**, 1070 (2009).
[6] H. G. Kim, K. T. Kim, Int. J. Mechanical Sciences **42**, 1339 (2000).
[7] R. R. Manel, O. Jan, Engineering Fracture Mechanics **76**, 1485 (2009).
[8] P. Schade, Inter. J. Refractory Metals&Hard Mater **28**, 648 (2000).
[9] P. Schade, Inter. J. Refractory Metals&Hard Mater **24**, 332 (2006).
[10] W. F. Ma, H. C. Kou, C. S. Chen, J. S. Li, H. Chang, L. Zhou, H. Z. Fu, Mater. Sci. Eng. A **486**, 308 (2008).
[11] K. Q. Qiu, A. M. Wang, H. F. Zhang, B. Z. Ding, Z. Q. Hua, Intermetallics **10**, 1283 (2002).
[12] X. H. Yang, S. H. Liang, X. H. Wang, P. Xiao, Z. K. Fan, Inter. J. Refractory Metals & Hard. Mater. **28**, 305 (2010).
[13] J. G. Cheng, L. Wan, Y. B. Cai, J. C. Zhu, P. Song, J. Dong, J. Mater. Process. Tech. **1**, 137 (2010).
[14] S. H. Hong, B. K. Kim, Z. A. Munir, Mater. Sci. Eng. A **405**, 325 (2005).
[15] A. Ibrahim, M. Abdallah, S. F. Mostafa, A. A. Hegazy, Materials & Design **30**, 1398 (2009).
[16] F. Doré, S. Lay, N. Eustathopoulos, C.H. Allibert, Scripta Mater. **49**, 237 (2003).

*Corresponding author: zhangyangmath@163.com